Rare Metal Materials and Engineering
Volume 51, Issue 6, June 2022
Available online at www.rmme.ac.cn

Science Press

Cite this article as: Wang Xiangjie, Yang Lingfei, Tan Hongjuan, et al. Effect of Cooling Rate on Solidification Microstructure and Properties of Al-Cu Binary Alloy[J]. Rare Metal Materials and Engineering, 2022, 51(06): 2033-2038.

ARTICLE

Effect of Cooling Rate on Solidification Microstructure and Properties of Al-Cu Binary Alloy

Wang Xiangjie[1,2], Yang Lingfei[1,2], Tan Hongjuan[1,2], Yu Fang[1,2], Cui Jianzhong[1,2]

[1] Key Lab of Electromagnetic Processing of Materials, Ministry of Education, Northeastern University, Shenyang 110819, China; [2] Advanced Manufacturing Technology and Engineering Research Centers, Northeastern University, Shenyang 110819, China

Abstract: To investigate the influence of cooling rate on the solidification structure of Al-Cu binary alloy, the ingot of Al-6%Cu alloy was produced by the wedge-shaped copper mode casting. The results indicate that when the cooling rate decreases from 100 K/s to 2 K/s, the grain morphology transformation of ingot is as follows: columnar grains→mixing of columnar grains with equiaxed grains→ equiaxed grains. Meanwhile, the width of columnar crystal at the ingot edge increases from 244.7 μm to 408.2 μm, the average grain size of equiaxed crystal at the ingot core decreases from 629.8 μm to 152.8 μm, and the average dendrite arm spacing increases from 10.1 μm to 52.8 μm. The parameters A and n of Al-6%Cu alloy in the empirical formula of average dendrite arm spacing and cooling rate are 78.75 and 0.41, respectively. When the cooling rate decreases from 100 K/s to 25 K/s, the morphology of eutectic Al_2Cu changes from skeletal to lamellar, and α-Al near the eutectic Al_2Cu is cellular. With the cooling rate increases from 2 K/s to 100 K/s, the hardness of Al-6%Cu alloy is increased from 618 MPa to 726 MPa.

Key words: Al-Cu binary alloy; wedge-shaped copper mode casting; solidification microstructure; cooling rate; properties

Al-Cu alloys have been widely applied in aerospace and automotive fields due to their lower density and excellent mechanical properties[1-3]. In industrial production, different solidification structures of aluminum alloy have a significant impact on subsequent production and processing[4-6]. Varying cooling rates lead to different grain size morphology, dendrite arm spacing and eutectic phase morphology of the cast ingot. Some investigations indicate that increasing cooling rate leads to a decrease in the size of grain[7,8]. A variation in the cooling rate affects grain morphology and hence the mechanical properties of the alloy[9,10]. Long-term experience shows that mechanical properties of equiaxed crystal are superior to those of columnar crystals. Therefore, a large amount of research has been devoted to exploring the formation of equiaxed crystals and the mechanism of columnar crystal-equiaxed crystal transformation to obtain the solidification structure of completely equiaxed crystals[11-14].

When the hypoeutectic Al-Cu alloy is solidified, the primary phase α-Al tends to grow into dendrites, and eutectic constituents are formed between the dendrite arms. The change of cooling rate will lead to the change of the morphology and size of the second phase in the alloy. Under the influence of the cooling rate, large-sized eutectic phases sometimes appear in the cast alloy. It takes a long time for these precipitated phases to dissolve, which brings a lot of inconvenience to the subsequent heat treatment[15-17]. Dendrite arm spacing (DAS) is an important structural parameter that reflects the local solidification conditions. Because the dendritic structure reflects the local heat dissipation state during the solidification process, DAS is very sensitive to the cooling rate. Rontó et al[18,19] studied the effect of the cooling rate on the secondary dendrite arm spacing of Al-Mg-Si alloys. The industry usually uses the relationship between the cooling rate and the distance between the dendrite arms to estimate the cooling rate[20-22], as shown in Eq (1):

$$\mathrm{DAS} = AV_c^{-n} \quad (1)$$

where DAS is the dendrite arm spacing, V_c is the cooling rate, and A and n are alloy parameters. The values of A and n are

Received date: June 05, 2021
Foundation item: Fundamental Research Funds for the National Natural Science Foundation of China (U1708251); Key Research and Development Program of Liaoning (2020JH2/10700003); Liaoning Revitalization Talents Program, China (XLYC1807027); Fundamental Research Funds for the Central Universities (N2109004)
Corresponding author: Wang Xiangjie, Ph. D., Associate Professor, Key Lab of Electromagnetic Processing of Materials, Ministry of Education, Northeastern University, Shenyang 110819, Tel: 0086-24-83689561, E-mail: wangxj@epm.neu.edu.cn

correlated with the composition of the aluminum alloy. Many experiments have measured parameters A and n of alloys with different designs[19,23], which provide a reference for the determination of alloy cooling rate and the prediction of dendrite arm spacing.

In this study, the wedge-shaped copper mode casting was used for casting Al-6%Cu alloy. Current work was planned with two aims in mind. One of the aims is to investigate the effect of cooling rates on grain morphology, DAS, eutectic Al_2Cu and its nearby α-Al morphology of Al-6%Cu alloy. The second aim is to obtain reliable values for the coefficients in Eq. (1) for Al-6%Cu alloys solidified in the range of cooling rates from 2 K/s to 100 K/s. Al-Cu alloys are the most frequently used model alloys, and these data will be very helpful for both experimental and modeling work.

1 Experiment

To obtain Al-6%Cu alloys solidified at different cooling rates, the alloy was produced by the high-purity Al ingot and Cu ingot (99.99wt%) using the wedge-shaped copper mode casting. Firstly, a certain proportion of pure industrial aluminum and pure copper were put into the graphite crucible (preheated at 250 °C), and then the crucible was transferred to an intermediate frequency induction electric furnace for heating. After the molten metal temperature in the furnace reached 780 °C, keep it for 20 min and add a degassing agent (C_2Cl_6). After removing the oxide film and scum on the surface of the molten metal, the melt was cast into a wedge-shaped copper mold. The wedge-shaped copper mold casting mold is shown in Fig. 1a. Before casting, the thermocouple was set in the wedge-shaped copper mold, the cooling curve during solidification of the alloy was measured by a temperature recorder of the type LR8401-21 during the solidification processes, and the temperature acquisition time was 0.1 s.

Fig. 1a shows the internal structure of the wedge-shaped copper mold. The wedge-shaped mold is composed of two parts. The upper part is made of thermal insulation material, and the lower part is made of metal copper. The samples obtained by casting were cut at the middle position. The remainder of the ingot after cut was numbered as A, B, C, D. The temperature in the measurement position was recorded by K-thermocouples, as shown in Fig.1b.

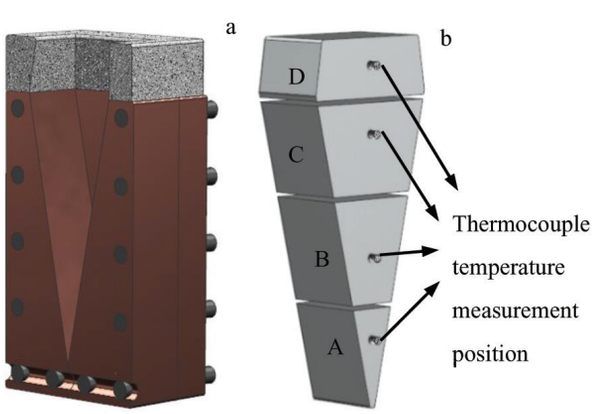

Fig.1 Schematic diagram of wedge-shaped copper mold (a) and sample temperature measurement point (b)

The as-cast specimen taken from a one-half radius region of cross section of ingots was anodized with 2.5vol% HBF_4 solution at a voltage of 20 V and a current of 0.5~1.0 mA for about 35 s and then the microstructure was observed by a Leica (Wetzlar, Germany) DMI5000M optical microscope with cross-polarized light. The samples were deeply etched with 10% NaOH solution and aqua regia at room temperature, and the corrosion time was 30 s. The morphology and elemental composition of the phases in the as-cast alloy were characterized by ultra plus field emission scanning electron microscope (Zeiss, Germany) equipped with X-ray spectroscope, and the area fraction of the eutectic structure in the SEM images was calculated by Image-Pro Plus (6.0, Media Cybernetics, Rockville, MD, USA). The cooling curve measured during the experiment is shown in Fig. 2. After calculation, the cooling rate is 100, 25, 10, and 2 K/s. For a sample solidified at a cooling rate, the area fractions of the eutectic phase in at least ten pictures at different positions were counted and the average value was taken to minimize statistical errors and make the experimental results representative. Cooling curves and the calculation results are shown in Fig. 2.

2 Results and Discussion

2.1 Effect of cooling rate on grain morphology and size

Fig. 3 shows the microscopic grain morphology of the four samples A, B, C, and D. The white mark position is the K-thermocouple temperature measurement position, and the side value is its cooling rate. In general, it can be observed that sample A is almost entirely composed of columnar crystals, samples B and C are composed of a mixture of columnar crystals and equiaxed crystals, and sample D is composed of equiaxed grains.

Comparing the direction 1 indicated by the arrow in Fig. 3, three samples A, B and C are columnar crystals if they are close to the mold wall. Preferred orientation of dendrites resulting in a columnar structure is parallel to the growth, in

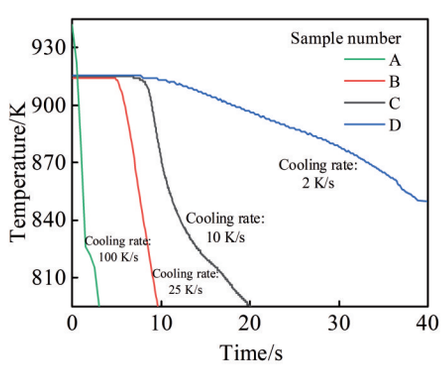

Fig.2 Cooling curves of different locations at different cooling rates

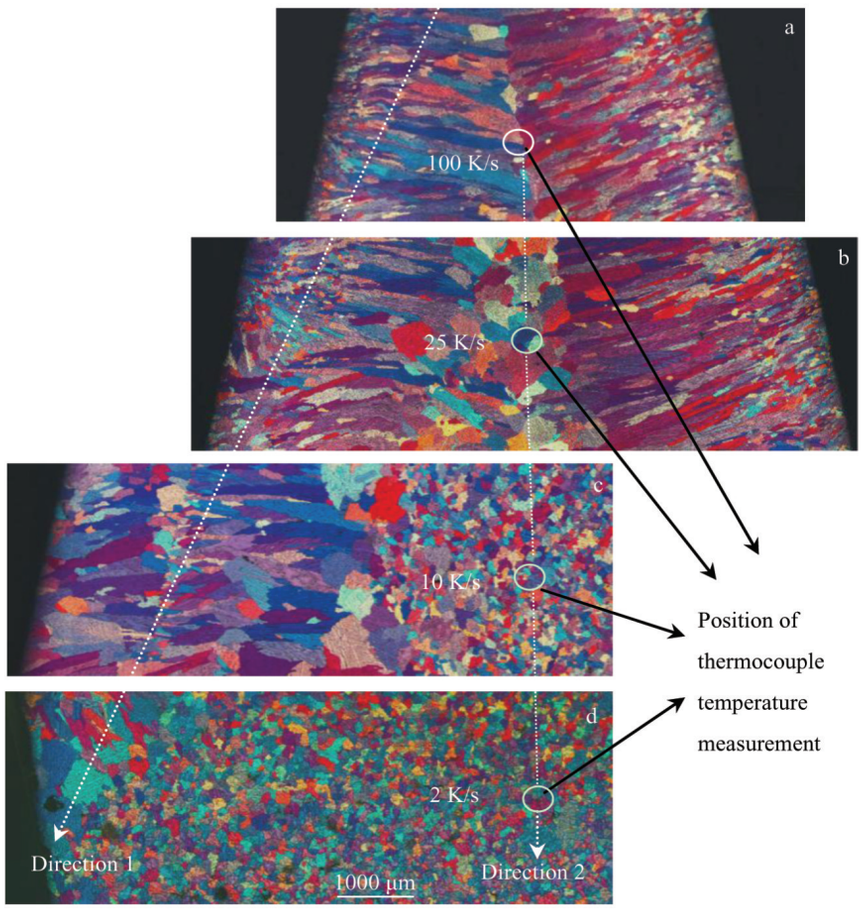

Fig.3 Grain morphologies of Al-6%Cu at different cooling rates: (a) sample A, 100 K/s; (b) sample B, 25 K/s; (c) sample C, 10 K/s; (d) sample D, 2 K/s

other words, the heat dissipation direction near the mold wall is perpendicular to the mold wall, and the growth rate of the crystal grains with the dendrite axis in this orientation is higher than that of the crystal grains with the dendrite axis in other orientations. Due to competitive growth, the dendrite axis is perpendicular to the grains on the die wall, squeezing out other grains. The columnar grains solidify in a preferred orientation so the long axis is parallel to the specific crystallographic direction [13]. Sample D is solidified at the insulation material, heat dissipation is slow and there is no specific fastest heat dissipation direction, and the crystal grains will not grow according to the preferred orientation, so there is no columnar crystal on the mold wall.

The columnar crystal widths of samples A, B, and C were counted by Image-Pro Plus software, and the results are shown in Table 1. It can be observed that as the cooling rate decreases, the columnar crystal width gradually increases from 244.7 μm to 408.2 μm. When the cooling rate decreases from 100 K/s to 25 K/s, the microstructure of the equiaxed crystals begins to appear in the ingot core (as shown in the direction 2 in Fig. 3). When the cooling rate continues to decrease to 2 K/s, the average grain size of the equiaxed crystal decreases from 629.8 μm to 152.8 μm.

Winegard et al[23] believed that when the component undercooling at the tip of the columnar grain exceeds the critical undercooling required for nucleation, equiaxed crystal nuclei will be formed in the melt. Some people believed that the broken dendritic fragments in the process of columnar crystal growth enter the center of the ingot through convection and become the core of equiaxed crystal nucleation [24]. These equiaxed crystal grains gather together to inhibit the growth of columnar crystals, so samples B and C form a mixed grain

Table 1 Grain size of Al-6%Cu alloy solidified at different cooling rates

Sample number	A		B		C		D	
Cooling rate/K·s^{-1}	100		25		10		2	
Grain morphology	Columnar crystal	Equiaxed crystal	Columnar crystal	Equiaxed crystal	Columnar crystal	Equiaxed crystal	Columnar crystal	Equiaxed crystal
Grain size/μm	244.7	0	352.3	629.8	408.2	219.8	0	152.8

structure of columnar crystals at the edge of the ingot and equiaxed crystals at the center.

2.2 Effect of cooling rate on DAS

Fig. 4 shows the microstructure of Al-6%Cu alloy at different cooling rates. It can be observed that when the cooling rate is reduced from 100 K/s to 2 K/s, the microstructure of the alloy is significantly coarsened. The DAS of Al-6%Cu alloys at different cooling rates was calculated. As shown in Fig. 5, when the cooling rate is reduced from 100 K/s to 2 K/s, the DAS increases from 10.1 μm to 52.8 μm.

Eq. (1) is frequently used for the estimation of the cooling rate from the structure data. According to the relationship between the cooling rate and the DAS, when the parameters A and n are determined, the cooling rate can be estimated from the DAS by Eq. (1). Regarding the Al-Cu alloy parameters A and n, different values for the parameters in Eq. (1) were reported in literature for Al-Cu binary alloy, and the collated data are shown in Table 2.

It can be seen from Table 2 that the Cu content has a more significant influence on the parameters A and n, and the parameters A and n are very different for Al-Cu alloys with different compositions. To obtain accurate and reliable parameters A and n of Al-6%Cu alloy, this study combines the experimental data obtained to calculate the relevant parameters of the alloy.

The values of parameters A and n were also calculated by relevant researches. Young et al[19] established the relationship between the parameter A and the mass percentage x of Cu in the Al-Cu binary alloy. According to the experimental data of Eskin[24]:

$$A=143.73x^{-0.356} \quad (2)$$

where x is the percentage of Cu in the alloy, A is the Al-Cu alloy constant. According to Eq. (2), the value of constant A of Al-6%Cu alloy is calculated to be 78.75, n is 0.41, and R^2 is 0.982.

As shown in Fig. 5, the calculation result is consistent with the relevant calculation result of this experiment, i. e. the higher the Cu content in the aluminum alloy, the smaller the value of A.

2.3 Effect of cooling rate on the morphology of eutectic Al_2Cu

Fig. 6 shows the microstructures of Al-6%Cu alloy solidified at cooling rates of 100 and 25 K/s. The upper left corner shows the eutectic Al_2Cu morphology after deep corrosion with NaOH solution. It can be observed that for samples at a cooling rate of 100 K/s, the eutectic Al_2Cu morphology is a skeleton and embedded in the aluminum matrix. When the cooling rate is reduced to 25 K/s, a lamellar morphology appears on the eutectic Al_2Cu. Since the sample solidified at 100 K/s has a high cooling rate and a significant degree of undercooling, the lamellar eutectic growth interface is unstable, so eutectic Al_2Cu forms this complex skeletal structure[25,26].

2.4 Morphology of α-Al near the eutectic Al_2Cu of Al-6%Cu alloy

Fig.7 shows the morphologies of Al-6%Cu alloys at cooling rates of 100 and 25 K/s after deep corrosion with aqua regia. It is found that there is a cellular structure near the eutectic Al_2Cu at a cooling rate of 25 K/s, while a similar cellular structure cannot be found in the sample at the cooling rate of 100 K/s. To determine the cellular composition, EDS analysis

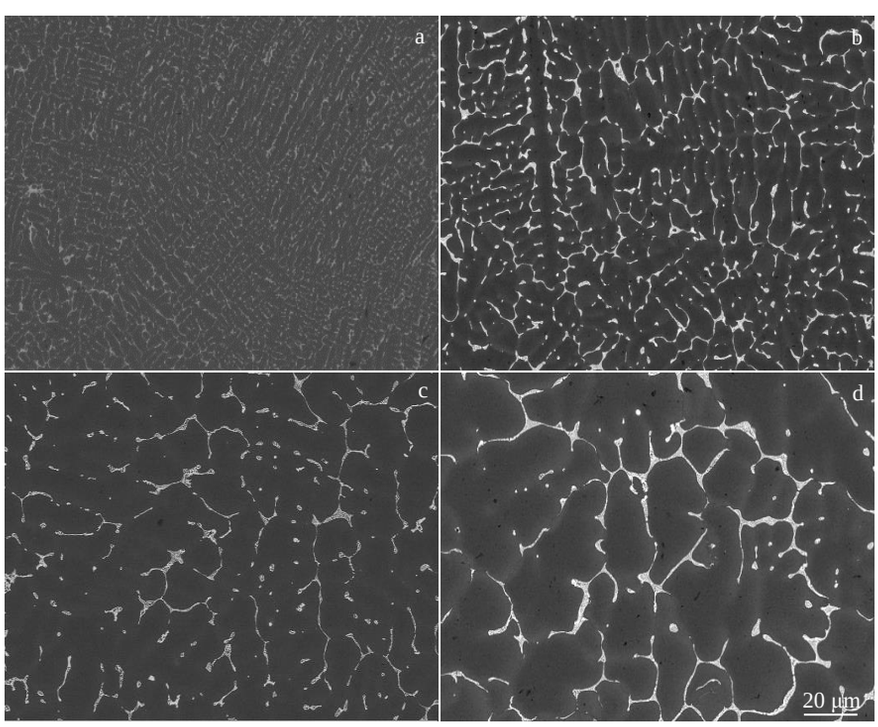

Fig.4 Microstructures of Al-6%Cu at the cooling rate of 100 K/s (a), 25 K/s (b), 10 K/s (c), and 2 K/s (d)

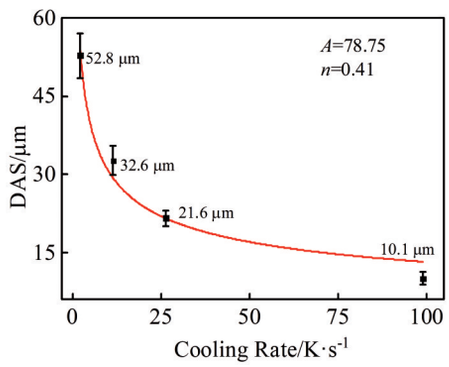

Fig.5 Variation of dendritic arm spacing of Al-6%Cu alloy at different cooling rates

Table 2 Parameters in Eq.(1) for Al-Cu binary alloy

Cu content/wt%	*A*	*n*
0.98[23]	144.7	0.44
2.12[23]	110.2	0.47
2.4[19]	1.2~5.9	0.23~0.38
3.24[23]	94.4	0.4
4.3[23]	85.6	0.41
4.4[19]	2.6~5.0	0.23~0.37
10[19]	1.1~3.2	0.25~0.39

was performed and the position is shown in Fig. 7b. The results show that the Cu content is only 2.4wt%, and it can be inferred that the cellular morphology near the eutectic Al_2Cu is α-Al. Thus, the eutectic constituent of Al-6%Cu alloy is composed of α-Al and Al_2Cu phases.

During the solidification and growth process, the Al atoms and Cu atoms existing in the front of the two-phase interface undergo short-range separation and diffusion in the liquid phase. When the liquid phase undergoes a eutectic reaction, the interface of the sample at a cooling rate of 25 K/s advances in a cellular shape, and the two phases of α-Al and Al_2Cu grow together. Finally, the lamellar eutectic structure forms, as shown in Fig. 7b. After aqua regia corrodes the eutectic Al_2Cu, the α-Al underneath seems cellular.

2.5 Effect of cooling rate on properties

Fig. 8 shows the hardness evolution of Al-6%Cu with different cooling rates. Cooling rate usually has a positively influence on the hardness[27]. The hardness of Al-6%Cu increases as cooling rate increases. When the cooling rate is 2 K/s, the hardness is 618 MPa, and when the cooling rate is 100 K/s, the hardness is 726 MPa. As the cooling rate increases, the more the phases and grains, the more the phase boundaries and grain boundaries, the larger the resistance encountered in the dislocation process, and the higher the hardness of the alloy. Meanwhile, Al-6%Cu hypoeutectic grain size is refined, finer eutectic Al_2Cu and DAS also produce a positive effect on hardness.

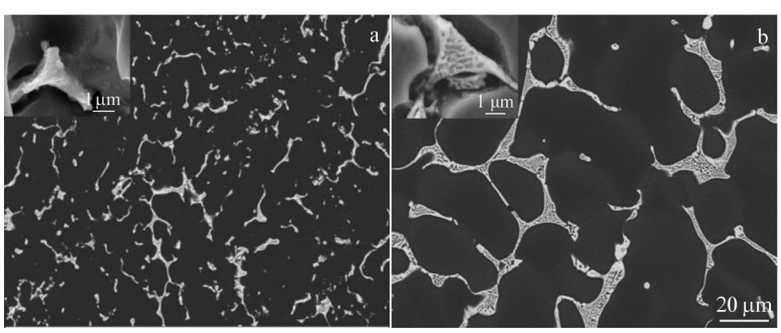

Fig.6 Morphologies of eutectic Al_2Cu at the cooling rate of 100 K/s (a) and 25 K/s (b)

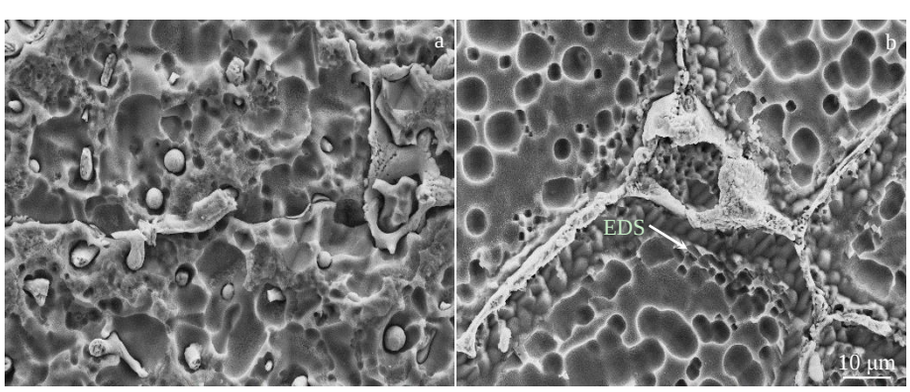

Fig.7 Morphologies of Al-6%Cu alloy after deep corrosion with aqua regia at the cooling rates of 100 K/s (a) and 25 K/s (b)

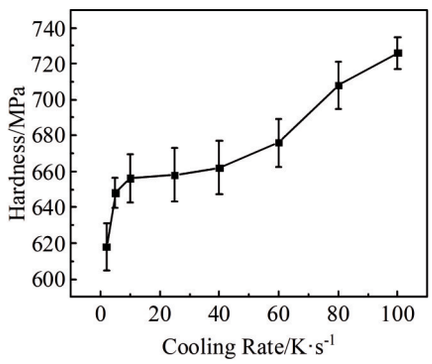

Fig.8 Hardness of Al-6%Cu alloy at different cooling rates

3 Conclusions

1) As the cooling rate decreases, the grain shape transformation of Al-6%Cu alloys is: columnar crystals→mixing of columnar crystals and equiaxed crystals→equiaxed crystals. The columnar crystal width increases from 244.7 μm to 408.2 μm, and the average grain size of the equiaxed crystal is reduced from 629.8 μm to 152.8 μm.

2) When the cooling rate is reduced from 100 K/s to 2 K/s, the DAS is increased from 10.1 μm to 52.8 μm; the values of parameters A and n for the Al-6%Cu alloy are calculated to be 78.75 and 0.41, respectively.

3) The morphology of eutectic Al_2Cu in Al-6%Cu alloy changes from skeletal to lamellar as the cooling rate decreases from 100 K/s to 25 K/s.

4) The α-Al morphology near the eutectic Al_2Cu is cellular at a cooling rate of 25 K/s.

5) As the cooling rate increases from 2 K/s to 100 K/s, the hardness of Al-6%Cu alloy increases from 618 MPa to 726 MPa.

References

1 Frank G, Matha G. *Science*[J], 1994, 266(5187): 1015
2 Kasperovich G, Volkmann T, Ratke L *et al. Metallurgical and Materials Transactions A*[J], 2008, 39(5): 1183
3 Mirshahi F, Meratian M, Panjepour M. *Materials Science and Engineering A*[J], 2011, 528(29-30): 8319
4 Lin Yaojun, Mao Shuaiying, Yan Zhigang *et al. Materials Science and Engineering A*[J], 2017, 692(24):182
5 Zhang Yue, Du Wenbo, Li Shubo *et al. Rare Metal Materials and Engineering*[J], 2018, 47(10): 3120 (in Chinese)
6 Zhu Dongdong, Dong Duo, Zhou Zhaozhong *et al. Rare Metal Materials and Engineering*[J], 2016, 45(7): 1745 (in Chinese)
7 Sheng L Y, Guo J T, Ye H Q. *Materials and Design*[J], 2009, 30(4): 964 (in Chinese)
8 Spittle J A. *International Materials Reviews*[J], 2006, 51(4): 247
9 Zhang L Y, Jiang Y H, Ma Z *et al. Journal of Materials Processing Technology*[J], 2008, 207(1-3): 107
10 Mathiesen R H, Arnberg L, Bleuet P *et al. Metallurgical and Materials Transactions A*[J], 2006, 37(8): 2515
11 Ahmadein M, Wu M, Ludwig A J. *Journal of Crystal Growth*[J], 2015, 417(1): 65
12 Wu Menghuai, Domitner Josef, Ludwig Andreas. *Metallurgical and Materials Transactions A*[J], 2012, 43(3): 945
13 Yao X, Wang H, He B *et al. Materials Science Forum*[J], 2005(475-479): 3141
14 Tiller W A, Jackson K A, Rutter J W *et al. Acta Metallurgica*[J], 1953, 1(4): 428
15 Flemings M C. *Metallurgical Transactions*[J], 1974, 5(10): 2121
16 Sarreal J A, Abbaschian G J. *Metallurgical Transactions A*[J], 1986, 17(11): 2063
17 Rontó V, Roósz A. *International Journal of Cast Metals Research*[J], 2001, 13(6): 337
18 Rontó V, Roósz A. *International Journal of Cast Metals Research*[J], 2001, 14(2): 131
19 Young K P, Kerkwood D H. *Metallurgical Transactions A*[J], 1975, 6(1): 197
20 Singh J, Chauhan A. *Journal of Materials Research and Technology*[J], 2016, 5(2): 159
21 Gupta M, Karunasiri G, Lai M O. *Materials Science and Engineering A* [J], 1996, 219(1-2): 133
22 Cho J I, Kim C W. *International Journal of Metalcasting*[J], 2014, 8(1): 49
23 Winegard W C, Majka S, Thall B M *et al. Applied Mechanics and Materials*[J], 1951, 29(4): 320
24 Eskin D, Du Q, Ruvalcabax D *et al. Materials Science and Engineering A*[J], 2005, 405(1-2): 1
25 Tourret D, Gandin C A. *Acta Materialia*[J], 2009, 57(7): 2066
26 Das A, Mittemeijer E J. *Metallurgical and Materials Transactions A*[J], 2000, 31(8): 2049
27 Pu Cunji, Xie Ming, Du Wenjia *et al. Rare Metal Materials and Engineering*[J], 2015, 44(4): 1012 (in Chinese)

冷却速率对 Al-Cu 二元合金凝固组织和性能的影响

王向杰[1,2]，杨凌飞[1,2]，谭宏娟[1,2]，于 芳[1,2]，崔建忠[1,2]

(1. 东北大学 材料电磁过程研究教育部重点实验室，辽宁 沈阳 110819)

(2. 东北大学 材料先进制备技术教育部工程研究中心，辽宁 沈阳 110819)

摘 要：为了研究冷却速率对 Al-Cu 二元合金凝固组织和性能的影响，通过楔形铜模铸造制备了 Al-6%Cu 合金铸锭。结果表明，当冷却速率从 100 K/s 降低到 2 K/s 时，铸锭晶粒形态的转变过程为：全部柱状晶→柱状晶与等轴晶混合→全部等轴晶。同时，靠近模壁处的柱状晶宽度从 244.7 μm 增加到 408.2 μm，铸锭心部等轴晶的平均晶粒尺寸从 629.8 μm 减小到 152.8 μm，并且平均枝晶臂间距从 10.1 μm 增加到 52.8 μm。计算得出 Al-6%Cu 合金平均枝晶臂间距和冷却速率经验公式中的参数，其中 A 和 n 的值分别为 78.75 和 0.41。当冷却速率从 100 K/s 降低到 25 K/s 时，共晶 Al_2Cu 的形态从骨骼状变为片层状，在共晶 Al_2Cu 附近的 α-Al 的形态呈蜂窝状。当冷却速率由 2 K/s 增加到 100 K/s 时，Al-6%Cu 合金的硬度由 618 MPa 增加到 726 MPa。

关键词：Al-Cu 二元合金；楔形铜模铸造；凝固组织；冷却速率；性能

作者简介：王向杰，男，1982 年生，博士，副教授，东北大学材料电磁过程研究教育部重点实验室，辽宁 沈阳 110819，电话：024-83689561，E-mail：wangxj@epm.neu.edu.cn